Cohesion influences on erosion and bed load transport

Rajesh K. Jain[1] and Umesh C. Kothyari[1]

Received 30 March 2008; revised 13 March 2009; accepted 27 March 2009; published 11 June 2009.

[1] Studies on erosion and transport rates of cohesive sediment mixtures containing gravel are not reported so far in the literature to the best of our knowledge. Results from laboratory experiments on the process of erosion of cohesive sediment mixtures by open-channel flow are presented. The sediment used for experimentation consisted of fine gravel mixed with clay in proportions varying from 10% to 50% and fine gravel, fine sand in equal proportion (by weight) mixed with clay proportions again varying from 10% to 50% by weight. Experimental observations have revealed that the process of detachment of cohesive sediment mixtures containing gravel is significantly different from that of cohesionless sediments. Also, it is different from the detachment process of cohesive sediment mixtures not containing coarser-size material. Experimental data on transport rates of the bed load of the cohesive sediment mixtures are presented. On the basis of dimensional considerations, a computational procedure is proposed to determine the bed load transport rates generated from erosion of the different size fractions of sediment mixtures. Clay percentage and unconfined compressive strength of the sediment bed were the main parameters controlling bed load transport rate of such sediments. In the absence of cohesion, the proposed method reduces to the Patel and Ranga Raju (1996) method for bed load transport rate computation of nonuniform cohesionless sediments.

Citation: Jain, R. K., and U. C. Kothyari (2009), Cohesion influences on erosion and bed load transport, *Water Resour. Res.*, *45*, W06410, doi:10.1029/2008WR007044.

1. Introduction

[2] Assessment of cohesive sediment erosion and transport rate by the flow of water is the topic of primary importance for many hydraulic engineering-related tasks like mitigation of soil erosion in the catchment areas, studies on reservoir sedimentation, stable channel design, and river morphological modeling. This topic is also important for ecological investigations since cohesive sediment affects the heath of aquatic ecosystem by degrading water clarity and transporting pollutants [*Aberle et al.*, 2006]. The process of cohesive sediment erosion and transport also influences the effects of fine sediment deposition within the riverbed material on aquatic life and also engineering project investigations like stream bank erosion and stability, scouring around the obstructions in the flow, etc.

[3] The processes of bed load and suspended load transport for cohesionless uniform and nonuniform sediments are reasonably well understood [*Garde and Ranga Raju*, 2006]. Similarly, several investigations are also available on the process of erosion and transport of consolidated and unconsolidated uniform size cohesive sediments such as clays [*Raudikivi*, 1990]. However, in nature, the catchment land surface and river bed material frequently consist of the mixture of cohesive as well as cohesionless sediments like mixtures of sand, gravel, and clay, etc. Soil in the upland catchment areas is one of the examples of this type of sediment [*Kothyari and Jain*, 2008]. For instance, fan delta bed slopes of Britannia Beach, British Columbia, dominantly consist of mixture of clay and gravel [*Prior and Bornhold*, 1986]. Clay-sand-gravel mixtures, however, naturally occur in several geologies [*van Rijn*, 2007]. Thus the erosion of the beds of sand, gravel, and clay mixture by the river flow is a problem of considerable importance in the field of Earth sciences and engineering. The process of erosion and transport of sediment mixtures consisting of clay and coarser cohesionless sediment like gravel by the flow is a topic yet to be explored by the researchers. This topic therefore has been investigated in the present study.

[4] For cohesionless sediments, the main resistance to erosion is provided by submerged weight of sediment, but in cohesive beds the net attractive interparticle surface forces, frictional interlocking of grain aggregates, and electrochemical forces control the resistance to erosion and detachment. These forces vary with the type of clay, antecedent moisture conditions, type of shear application, and drainage conditions [*Ansari et al.*, 2003]. As a result these forces are not yet understood completely. The main mechanisms that cause sediment to be moved in flowing water are the velocity of flow and shear and normal stress resulting from flow turbulence [e.g., *Garde and Ranga Raju*, 2006]. When the hydrodynamic force in a turbulent flow exceeds the resisting force of a cohesive sediment bed, the sediment starts getting detached from the bed and the flowing water becomes turbid. This stage is characterized by the initiation of erosion [*Kothyari and Jain*, 2008]. With further increase in shear stress by the flow, the sediment is detached from the bed and is transported by the flow. In

[1]Department of Civil Engineering, Indian Institute of Technology Roorkee, Roorkee, India.

0043-1397/09/2008WR007044$09.00

present investigation the effect of the presence of cohesive material (clay) on the process of erosion and bed load transport of the detached sediment, namely, fine gravel and sand, is studied.

2. Brief Review

[5] Numerous investigations related to erosion and transport rate of uniform and nonuniform sediments in the absence of cohesion are available [*Garde and Ranga Raju*, 2006]. However, detailed investigations have not been carried out as yet for the determination of erosion of sediments having gravel and clay size also present in it. A few investigators, however, have studied through use of laboratory-based experiments the erosion of cohesive sediments that mostly consisted of either pure clay or mixtures of sand, silt, and clay. In most of these studies erosion rate of the cohesive sediment mixtures was measured volumetrically or by weighing the material lost by the erosion process. The mode of transport (in the form of bed or suspended load), however, was not mentioned. Several studies on simultaneous erosion and deposition of cohesive sediments are available in the literature [*Partheniades*, 1962, 1965, 1966; *Zreik et al.*, 1998; *Aberle et al.*, 2004]. In the present study, however, we present only the review of the studies on detachment and erosion of the cohesive sediments.

[6] *Grissinger* [1966] studied the erosion rate of cohesive sediments consisting of different clay minerals such as illite, kaolinite, etc. The rate of erosion of molded clay sample subjected to a uniform erosive force was measured, and the influence of concentration of clay minerals, bulk density, clay particle orientation, and antecedent moisture content on the erosion rate was studied. *Partheniades and Passwell* [1970] conducted experiments on erosion of fine cohesive sediments and concluded that surface erosion is controlled by the strength of interparticular bonds. *Arulanandan* [1975] measured erodibility of kaolinite, illite, and montmorillonite clay mixed with silica flour and reported that erodibility of soil depends on salt concentration of eroding fluid, and it decreases with the increasing salt concentration. *Grissinger et al.* [1981] measured erodibility of the stream bank material (sand-silt-clay) and observed the erosion rates to be significantly related to clay content of the sample.

[7] The erosion rate was reported to decrease as the clay content increases. Dispersive tendencies of clay, however, were reported not to have any effect on the erosion rate. *Shaikh et al.* [1988] measured the erosion rates of unsaturated compacted sodium (Na) and calcium (Ca) montmorillonite clays under a large range of tractive shear stress. They also proposed empirical equations to estimate the erosion rates of compacted unsaturated clays as a function of sodium adsorption ratio (SAR) and tractive stress. The erosion rates of nondispersive clay were reported to be 2 orders of magnitude higher than that of dispersive clay. *Hanson* [1990] measured erodibility of four sediments having different percentages of clay-silt-sand in it under high tractive shear stress due to the flow. The sediment that had higher sand content and lower clay content were noticed to have more erodibility than the sediment that had lower sand content and higher clay content. *Hanson and Robinson* [1993] conducted a compaction-based study to determine the influence of density and moisture content on erodibility. Sediment samples (mixture of clay-silt-sand) were prepared by methods using dynamic compaction and static compaction. Erosion resistance was found to increase with an increase in the moisture content and dry unit weight of the sediment sample. *Temple and Hanson* [1994] studied the erosion rate of cohesive sediments to improve the criteria for design and analysis of vegetated earth spillways. They proposed a relationship for the determination of the erosion rate coefficient in terms of percent clay, its dry unit weight, and specific weight of the fluid. Strong correlation was noticed between the erosion rates of cohesive sediments and the shear stress due to the flow.

[8] *Robinson and Hanson* [1995] studied the effect of compaction on the head-cut erosion process. They tested two types of soil, i.e., red sandy clay soil and silty sand. The soils were compacted in horizontal layers at predetermined values of moisture content and density. The head-cut advance rate was also found to decrease with an increase in average dry density and unconfined compressive strength of sediment bed. *Parker et al.* [1995] studied the effect of compaction, strength, moisture content, and air entrapment on erodibility. The erosion rates of clay-silt-sand mixtures were observed to increase with an increase in the air entrapment and decrease with an increase in initial moisture content. *Jepsen et al.* [1997] and *Roberts et al.* [1998] noticed the erosion resistance to increase with an increase in the bulk density for homogeneous cohesive sediment beds. *Amos et al.* [1997] and *Torfs* [1997], however, reported the erosion resistance to be independent of the bulk density for cohesive sediment beds composed of larger size particles, and that it was a function of the grain size only. Thus, for sediments composed of mud-sand mixture, the bed material also plays an important role in addition to the bulk density of the sediment [*Mitchener and Torfs*, 1996; *Houwing*, 1999].

[9] *Simon and Collison* [2001] measured pore water pressures below the cohesive beds in natural streams and in laboratory channels. These investigations revealed the presence of positive and negative pore water pressure to significantly affect the erosion in cohesive sediment beds. *Wan and Fell* [2004] concluded that depending upon the cohesive sediment properties, the erosion rates could differ by the order of up to 10^6 times for different cohesive sediments.

[10] A few investigators have also studied the erosion of cohesive sediments due to local scour under jets or by obstructions to the flow like bridge piers. These studies are useful in identification of the cohesive bed parameters controlling the rate of erosion and therefore are also reviewed next.

[11] *Moore and Masch* [1962] were among the first to investigate the clay erodibility by measuring the depth of scouring of horizontal clay sample subject to erosion by a submerged jet. A scouring index was used as erosion criterion, which is a dimensionless coefficient relating erosion depth and time. *Kuti and Yen* [1976] experimentally determined the erosion of cohesive sediment consisting of sand and clay minerals, placed downstream of a spillway. They noticed the volume of eroded material to decrease with an increase in the clay content of the sediment bed. *Abt and Ruff* [1982] carried out experiments to study the process

of culvert scour in cohesive sediment consisting of clay-silt-sand. They proposed empirical relationships for scour depth and scour volume as the functions of jet characteristics, discharge, and sediment parameters. *Briaud et al.* [1999, 2001] developed an apparatus known as the erosion function apparatus (EFA) to measure the erosion function of cohesive and cohesionless soil. This erosion function relates the erosion rate of soil samples to the flow shear stress. The EFA was used to measure the critical shear stress corresponding to the initiation of motion and the erosion rate beyond that point. *Briaud et al.* [2001] observed a poor correlation among the parameters describing the cohesive soil erodibility and the soil properties such as plasticity index, undrained shear strength, and percent passing a 0.075-mm sieve. They reported, however, a better correlation between the critical shear stress and the erodibility of the sediment sample. *Ting et al.* [2001] studied local scour at circular piers founded on clay. The experiments were conducted on three types of clay beds ranging from low-plasticity clay to high-plasticity clay. They proposed an equation to express pier scour depth and scour hole shape in clay, as a function of the pier Reynolds number. *Ansari et al.* [2003] studied the variation of maximum depth and volume of scour by submerged vertical jet in clay-sand mixtures. They proposed empirical relationships to compute maximum depth of scour and maximum volume of scour for nonplastic and plastic cohesive sediment as a function of dimensionless clay content, antecedent moisture content, and dry density. *Dey and Westrich* [2003] conducted experiments to study temporal variation of the scour depth in a cohesive bed downstream of an apron due to a submerged horizontal jet. The cohesive bed tested was made up of the natural sediments taken from the bed of river Neckar, Germany. The scour profiles at different times were noticed to follow a particular geometry that could be expressed in terms of a polynomial. *Mazurek et al.* [2003] measured the depth of scour of cohesive sediment bed by submerged plane turbulent wall jet. Using dimensional analysis, they proposed empirical equations to compute the maximum scour depth, location of maximum scour depth, and length of the scour hole at equilibrium conditions, which were related to the hydraulic properties of jet, nozzle thickness, and critical shear stress of the cohesive sediment.

[12] *Hanson and Hunt* [2006] conducted the jet erosion tests on two types of sediments: silty sand and lean clay to measure the effect of compaction on the erodibility. The sediment gradation and compaction water content were reported to have a vital control on erodibility. The erodibility was noticed to decrease with an increase in the dry density but at faster rate on the dry side of optimum water content than on the wet side.

[13] The review presented above has indicated that erodibility of the clay or sand-silt clay mixtures is dependent on several parameters like clay percentage, type of clay, compaction water content of cohesive sediment, gradation, plasticity index, air entrapment, undrained shear strength, dry density, and unconfined compressive strength of the sediment bed, etc., as well as the type of shear application. The review, however, indicates that investigations are not readily available as yet for the quantification of the influence of cohesion on the process of erosion and transport of nonuniform cohesive sediments having gravel sizes also present in the mixture.

3. Methods

[14] An extensive experimental program was undertaken to study the influence of cohesion on the process of erosion and transport of sediment mixtures with clay material present in it. These experiments were conducted in the Hydraulic Engineering Laboratory of the Department of Civil Engineering, Indian Institute of Technology, Roorkee, India. Details of these are given below.

3.1. Flume

[15] The experiments were conducted in a tilting flume 16 m long, 0.75 m wide, and 0.5 m deep. The channel had a test section of 6.0 m length, 0.75 m width, and 0.13 m depth starting at a distance of 8.0 m from channel entrance. Observations were made at various slopes of flume ranging from 2.417×10^{-3} to 1.0×10^{-2}. The details of the experimental procedure followed are given by *Kothyari and Jain* [2008]. Only the pertinent description, however, is repeated herein for completeness.

3.2. Sediment

[16] Cohesionless sediments consisting of fine sand and fine gravel were used as base sediment. The clay was added in various proportions to the base sediment to create cohesive sediments. In engineering applications the cohesive properties are considered as important, while the clay fraction in the sediment mixture is larger than about 5–10% [*van Ledden et al.*, 2004; *van Rijn*, 2007]. The cohesive sediments were therefore prepared by mixing clay materials in proportions varying from 10% to 50% with fine gravel and with fine sand/fine gravel mixtures (each in equal proportion by weight). The clay material had a median size d_{50} equal to 0.0039 mm and a geometric standard deviation σ_g equal to 1.5; sand had a median size d_{50} of 0.23 mm and σ_g of 1.53; while gravel had a median size d_{50} of 3.1 mm and σ_g of 1.28. The relative density of sand and gravel was 2.65. A wide range of field conditions were simulated by varying the antecedent conditions of thusly formed cohesive sediments. Experiments were also conducted to determine various engineering properties of clay, sand, and gravel and their mixtures and are described in detail by *Kothyari and Jain* [2008] and *Jain* [2008].

[17] The unconfined compressive strength of the sediments was measured by using laboratory-based unconfined compression test apparatus. Cylindrical specimen were taken from the compacted bed and tested as per *Bureau of Indian Standards* [1991] in unconfined compression apparatus. The bulk unit weight of sediment was determined as per *Bureau of Indian Standards* [1975] by using standard core cutter method. The value of dry density was computed by using the observed value of bulk density and antecedent moisture content. The void ratio is derived from computed value of dry density of cohesive sediments.

[18] The experiments were conducted on two types of bed material, namely, (1) the clay is mixed in varying proportions to uniform size gravel, and (2) the clay mixed in varying proportion to nonuniform sediment mixture consisting of sand and gravel mixed in equal percentages by

Table 1. Range of Sediment and Hydraulic Parameters for Clay-Gravel Mixtures[a]

P_{co} (%)	W (%)	γ_d (KN/m^3)	e ( )	UCS (KN/m^2)	h (m)	U (m/s)	S_f ( )	τ_o' (N/m^2)	Q_{Bg} (N/m-s)	Duration of Run (min)
10	4.88–10.42	16.00–17.98	0.443–0.622	0.0	0.0742–0.1449	0.575–0.813	0.0022–0.0078	2.247–4.179	0.0073–0.4318	150–570
20	6.64–15.38	17.23–18.75	0.381–0.503	0.0–6.38	0.0718–0.1554	0.685–1.03	0.0019–0.0068	2.546–5.554	0.005–0.4729	180–540
30	9.83–17.85	17.17–19.12	0.352–0.505	0.0–21.38	0.0856–0.1506	0.659–1.127	0.0021–0.0087	2.268–6.543	0.0079–0.4587	240–720
40	12.18–19.6	16.31–18.11	0.425–0.582	0.0–25.26	0.0697–0.1347	0.683–1.132	0.0025–0.0096	2.629–6.525	0.006–0.2375	420–900
50	12.17–21.52	15.08–18.74	0.374–0.708	0.0–46.7	0.0665–0.1555	0.651–1.226	0.0018–0.0101	1.953–7.129	0.0105–0.302	180–630

[a]P_{co} is initial clay percentage in the sediment bed, W is antecedent moisture content, γ_d is dry density, e is void ratio, UCS is unconfined compressive strength of sediment mixture, h is flow depth, U is mean velocity of flow, S_f is energy slope, τ_o' is grain shear stress of flow, and Q_{Bg} is bed load transport rate of gravel by erosion.

weight. Experiments were carried out under a range of antecedent moisture content and under different flow tractive shear stress values. For the quantification of the compaction of sediment bed, the initial dry density and initial value of cohesion represented by unconfined compression strength (UCS) [*Terzaghi et al.*, 1996] were measured.

3.3. Cohesive Sediment Transport Rate Measurements

[19] After saturating the sediment bed for 24 h the desired discharge was allowed into the flume and uniform flow was established simultaneously by maintaining the predetermined opening of the tailgate. The sediment being transported as bed load was collected in a trap at the downstream end of the flume. Bed load measurement was taken at regular interval of 15 min duration. Only cohesionless sediment of the bed material mixture moved as bed load. Cohesive sediment, i.e., clay, always moved as suspended load. The observations on the bed load only are reported herein. The collected sediment in the trap was weighed and converted into dry weight transport rate by applying a wetness correction factor that was determined through a priori calibration for each size of the mixture. Water and bed surface levels were also recorded simultaneously while bed degradation progressed. The water surface profile was measured with the help of pointer gauge having a least count of 0.1 mm resolution, and bed profile was measured using the gauge with a flat bottom (0.1 mm resolution). The flat-bottom gauge remained inside the flow only for very short durations while taking observations so as not to disturb the flow and bed conditions.

[20] The flow and bed surface profiles were recorded at a temporal interval of about 30 min for initial durations of the runs while the bed level degradation was fast. During later part of runs when bed transient became gradual, the water and bed surface profiles were recorded at an interval of about 60 min. Gauge readings for both water surface and channel bed elevations were made at longitudinal spacing of 0.5 m along the centerline of the flume. For reference, a few runs were also conducted without the presence of clay in the bed material. The total duration of any experimental run varied from 1 to 15 h. The average erosion rate was determined based on a number of samples of bed load transport taken during the periods while energy slope remained practically constant.

[21] A total of 46 runs were conducted with clay-gravel mixture whereas 48 runs were conducted for clay-sand-gravel mixture with clay percentages varying from 10% to 50%. The bed load measurements were made at regular time intervals. A total of 312 observations were taken for clay-gravel mixtures whereas 353 observations were taken for nonuniform sediment consisting of clay-sand-gravel mixtures. The ranges of specific conditions under which experimental data were collected are presented in Tables 1 and 2. The complete data are given by *Jain* [2008].

3.4. Variables Controlling Erosion and Bed Load Transport

[22] The erosion process of the cohesive sediments is controlled by their mechanical characteristics, like shear strength, and physicochemical properties. The amount and type of clay, antecedent moisture content, bulk density, unconfined compressive strength (UCS), etc., are therefore considered to be the easily measurable variables representing the factors controlling the erosion of cohesive sediments [*Kothyari and Jain*, 2008]. The effect of these variables on the transport rate of cohesive sediments produced through the process of erosion from channel bed is studied herein.

[23] The observations revealed that while a lower percentages of clay (up to 20%) was present in bed material, the sediment mostly moved by rolling of the particles. However, at higher clay percentages (above 20%) sediments were detached in the form of thick flakes from the bed surface, leaving longitudinal lines, which became significantly apparent on the bed surface by the end of the run (see Figure 1), representing the process of rill erosion in the catchment [*Kothyari et al.*, 1997]. Depending upon the antecedent moisture conditions and the flow shear stress applied, the sediment was detached by the flow in the form of lumps or chunks of the mixture of cohesive and cohesionless sediments of varying sizes and shapes. For still higher percentages of clay (i.e., 40% or more) the erosion occurred in the form of lumps of the cohesive sediment. These lumps were of irregular geometry and of different sizes too (see Figure 2, for example). Particularly at higher friction slopes and while clay proportion was about 50% in the bed material, bed load transport occurred mostly by removal of chunks of sediment from the bed surface leaving it with several potholes that eventually developed into a big pothole along the channel bed (see Figure 3) representing the gully erosion. However, during their transport the chunks got segregated into their constituents with clay invariably moving as suspended load and only sand and gravel mostly moving as the bed load.

[24] A comparison between the rate of bed load transport of cohesive and cohesionless sediments is made. The

Table 2. Range of Sediment and Hydraulic Parameters for Clay-Sand-Gravel Mixtures

P_{co} (%)	W (%)	γ_d (KN/m^3)	e ()	UCS (KN/m^2)	h (m)	U (m/s)	S_f ()	τ_o' (N/m^2)	Q_{Bg} (N/m-s)	Q_{Bs} [a] (N/m-s)	Duration of Run (min)
10	7.2–13.4	18.0–20.8	0.25–0.444	0.0	0.0851–0.1718	0.513–0.761	0.0014–0.0048	1.23–2.671	0.012–0.301	0.0029–0.0694	60–420
20	7.2–14.7	17.68–19.38	0.341–0.470	0.0–17.87	0.094–0.1792	0.552–1.016	0.0013–0.0061	1.48–4.52	0.007–0.381	0.0009–0.0634	240–780
30	7.42–21.69	16.27–19.01	0.368–0.598	0.0–23.19	0.0812–0.1759	0.539–1.056	0.001–0.0075	1.358–4.656	0.006–0.276	0.0011–0.046	240–435
40	10.28–19.54	16.05–18.39	0.414–0.62	0.0–25.18	0.078–0.1891	0.530–1.022	0.0014–0.0073	1.309–4.463	0.005–0.480	0.0005–0.0411	255–450
50	10.06–20.34	16.12–18.15	0.432–0.613	0.0–16.93	0.0585–0.1688	0.479–1.126	0.0013–0.0084	1.253–5.05	0.003–0.289	0.0007–0.0346	180–420

[a]Bed load transport rate of sand by erosion.

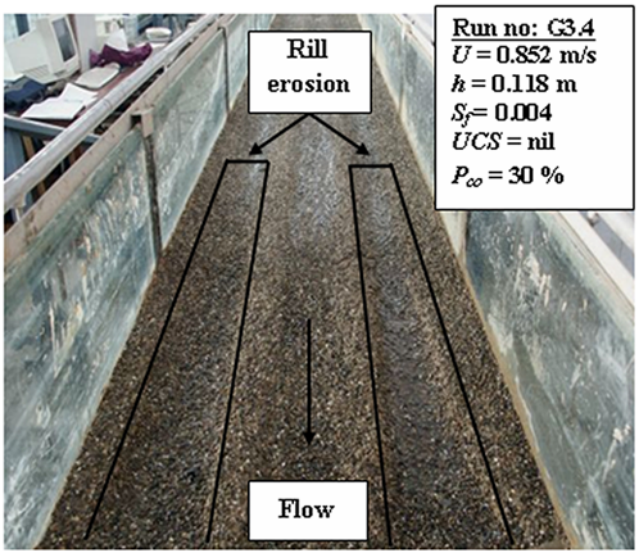

Figure 1. The erosion pattern in cohesive sediment-forming rill.

composition of bed materials and hence the transport rate of different size fractions present in them changed with time (details presented in sections 4.1 and 4.2) due to degradation of the channel bed. Figure 4 illustrates the temporal variation of rate of bed load transport of gravel in a few of the experimental runs using clay-gravel mixture. The temporal variation of rate of bed load transport of cohesionless sediment consisting of gravel alone is also given in Figure 4 for a comparison. The clay percentages present in bed material at the beginning of the experimental run as well as the flow conditions at the start of experimental run are also given in the Figure 4 for completeness. In Figure 4, P_{co} is initial percentage of clay in sediment bed, h is flow depth, U is mean velocity of flow, and S_o is channel bed slope. Similarly, Figure 5 illustrates the temporal variation of rate of bed load transport of sand and gravel sizes present in sand-gravel mixture and in clay-sand-gravel mixture for a few of the experimental runs. Figures 4 and 5 indeed reveal that the rate of bed load transport reduced manyfold

Figure 2. Sediment detached in the form of lumps of cohesive sediments of varying shapes and sizes.

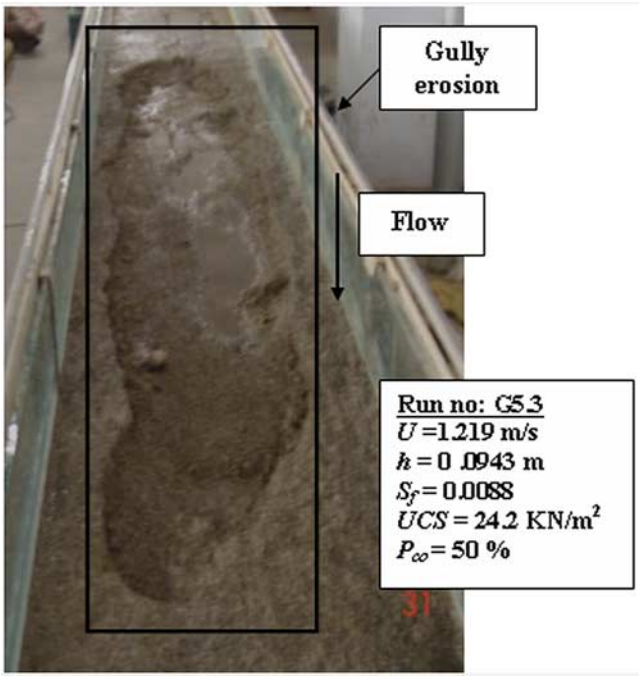

Figure 3. Erosion resulting in formation of big pothole (gully) along the flow length.

(twofold to more than tenfold) while clay in different percentages was present in the bed material. Figure 6 similarly illustrates temporal variation of the rate of bed load transport of gravel and sand size sediments for clay-gravel and clay-sand-gravel mixtures having varying values of the unconfined compressive strength (UCS) while the clay percentage at start of experimental runs in the bed material was same. Approximately similar flow conditions existed at the start of all the experimental runs plotted in Figure 6. Figure 6 also reveals that the bed load transport of sand and gravel size sediments reduced by manyfold even while UCS value of the sediment bed increased by a small amount. Such observations are consistent with the findings of *Kamphuis and Hall* [1983] and *Robinson and Hanson* [1995] on erosion of clay-sand mixtures. Thus a different level of cohesion makes a significant difference in the bed load transport and under similar flow conditions and the rate of bed load transport of cohesive sediments is significantly smaller than the rate of bed load transport of such sediment sizes in the absence of cohesion. Figures 4–6 also reveal that amount of clay fraction present and UCS value of bed material are the main parameters controlling the variation in rate of bed load transport as a different level of cohesion makes a significant difference in the bed load transport. Therefore the influence of these parameters on bed load transport rate is quantified by subsequent analysis.

4. Analysis

4.1. Active Bed Layer and Its Thickness

[25] The erosion of cohesive sediment is controlled not only by the macroscopic physical properties of sediment such as its density but also by the interparticle bond strength and its fabric characteristics [*Mazurek et al.*, 2001]. The composition of bed material gets altered during the experimental runs because of the differential transport rates of the individual size fractions present in it. The concept of active bed layer therefore is used to compute the dynamic conditions of the composition of bed material in general and for determination of the clay percentage within the bed material in particular, during different stages of the experimental run. This concept is defined below.

[26] The sediment transport rates measured during the present study corresponded to degrading nonuniform size sediment beds. The concept of the active bed layer is therefore utilized to determine the composition of the bed material at different times of a particular experimental run [*Singh et al.*, 2004]. Continuous exchange of sediment particles present in bed and flow takes place during the process of sediment transport, which is limited to certain thickness of the top surface of channel bed. This thickness depends upon the sediment size, bed form characteristics (if present), and flow characteristics. This layer of bed material through which exchange of sediment particles takes place is termed as the active bed layer (ABL). The material below the ABL is termed as substrate. *Rahuel et al.* [1989] considered the ABL thickness to be a function of flow depth, whereas *Borah et al.* [1982], *Parker* [1990], and *Correia et al.* [1992] considered the ABL to be a function of particle size. *Niekerk et al.* [1992] related the ABL thickness to sediment size and shear stress of flow. N. K. Khullar et al. (Suspended wash load transport of non-uniform sediments, submitted to *Journal of Hydraulic Engineering,* 2009) combined these approaches to account for the bimodal

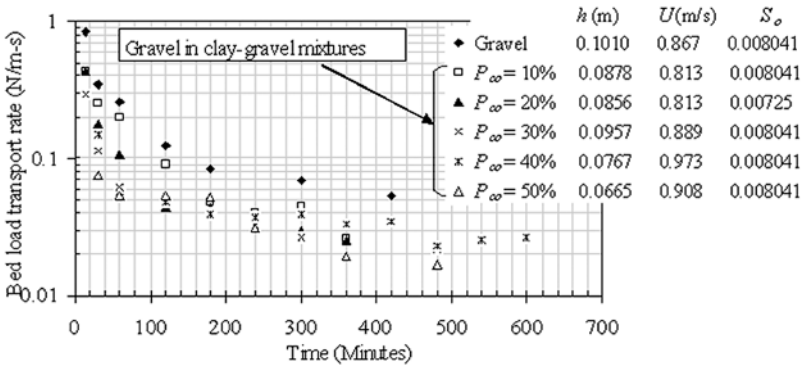

Figure 4. Variation of transport rate of gravel under various clay percentages in sediment bed for clay-gravel mixtures.

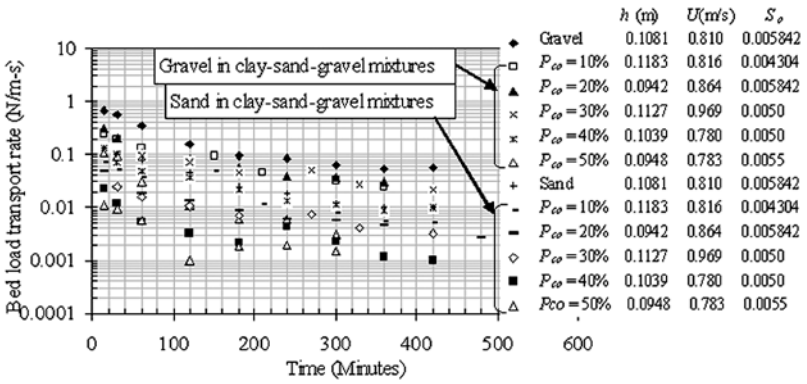

Figure 5. Variation of transport rate of sand and gravel under various clay percentages in sediment bed for clay-sand-gravel mixtures.

sediment mixtures, as also used in the present study, and proposed the following form of equation for the estimation of ABL thickness:

$$T_b = 0.3h\left(1 - \frac{\tau_{oc}}{\tau_o}\right) + 2d_{50}. \quad (1)$$

Here T_b is the active bed layer thickness, h is flow depth, d_{50} is the median sediment size, τ_{oc} is critical shear stress of cohesionless bed material, and τ_o is the average shear stress of flow. According to equation (1) when τ_{oc}/τ_o is small (for example, in dune regime), the thickness of ABL is mainly governed by the flow depth. However, when τ_{oc}/τ_o is close to unity, it is mainly related to the d_{50} size as in the case of flat bed conditions. The size d_{90} instead of d_{50} was used by *Singh et al.* [2004]. As mentioned above, equation (1) is also applicable to the bimodal sediment mixtures (N. K. Khullar et al., submitted manuscript, 2009).

[27] Initially both active bed layer and substrate are having the same composition. Thickness of the ABL is determined using equation (1) during the occurrence of erosion and transport process. For this, τ_{oc} appearing in equation (1) was replaced by the critical shear stress for cohesive sediments τ_{cc}. The relationship proposed by *Kothyari and Jain* [2008] is used to estimate τ_{cc} in equation (1). The volume of the sediment within the ABL corresponding to the fraction size d_i is computed as below:

$$V_{k,i} = T_b B \Delta x (1 - \lambda)(\Delta p_i / 100). \quad (2)$$

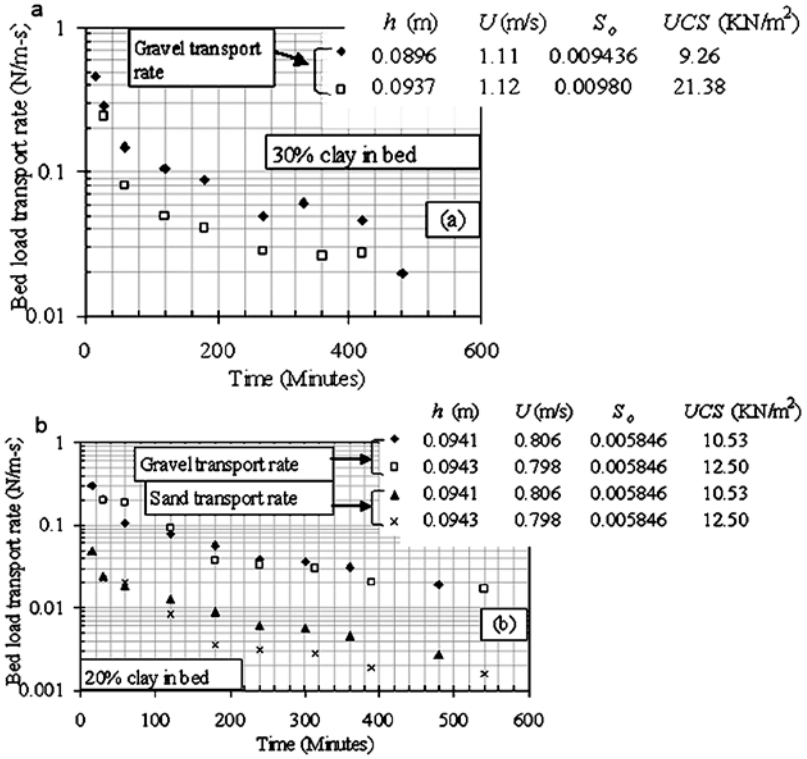

Figure 6. (a) Variation of gravel transport rate with unconfined compressive strength (UCS) for clay-gravel mixture. (b) Variation of sand and gravel transport rate with UCS for clay-sand-gravel mixture.

Here $V_{k,i}$ is the volume of sediment having size d_i at spatial position k, λ is the porosity of the bed material, Δp_i is the percentage of the sediment in the ABL having size d_i, B is the flow width, and Δx is spatial step for computations that was taken as equal to the length of the test section for computations by equation (2). The value of λ was estimated from the computed value of void ratio for a given experimental run, and it was assumed to remain constant for the entire duration of the experimental run.

4.2. Variation in the Composition of the ABL

[28] The composition of the ABL gets altered because of differential transport rates of the individual size fractions of the bed material. In the present case of degradation, the fractional part of ABL also gets eroded. The volume of various size fractions in remaining part of the ABL are computed using grain sorting equation as

$$V_{k+1,i}^{n+1} = V_{k+1,i}^{n} + \Delta t\left(Q_{bk,i}^{n+1} + Q_{sk,i}^{n+1} - Q_{bk+1,i}^{n+1} - Q_{sk+1,i}^{n+1}\right) + \Delta x\left(A_{k+1}^{n} C_{avk+1,i}^{n} - A_{k+1}^{n+1} C_{avk+1,i}^{n+1}\right). \quad (3)$$

Here $V_{k+1,i}$ represents the volume of ith size fraction in the ABL at spatial position $k + 1$, which now has thickness equal to T_b minus depth of degradation (computed from observed bed elevations) at the end of $n + 1$ time period during the experimental run, $Q_{bk+1,i}$ and $Q_{sk+1,i}$ are the volumetric bed load and suspended load sediment discharge, respectively, for ith size fraction at spatial position $k + 1$, A is the flow cross-sectional area, and $C_{avk+1,i}$ is average volumetric concentration of suspended load for ith size fraction at spatial position $k + 1$. As mentioned above Δx equal to the total length of test section was used in computations while Δt was taken as the time interval between the two consecutive observations of bed and water surface profiles. Therefore in equation (3) the observed values of $Q_{b,i}$, $Q_{s,i}$, and $C_{av,i}$ of different size fraction at the channel outlet (generated through erosion of cohesive sediment mixtures), at the given time level n, for a particular experimental run were used to compute the volume of the corresponding size fractions in the remaining part of the ABL. The form of equation (3) was originally used by *Borah et al.* [1982], *Karim and Kennedy* [1982], and *Singh et al.* [2004] for fraction-wise transport rate computation of nonuniform cohesionless sediment mixtures.

[29] Next the new thickness of the ABL is computed at the end of previous computational time step. Some part of the substrate now would join the ABL. The thickness of the part of substrate ΔT_s joining the ABL is computed using the following equation [*Singh et al.*, 2004]:

$$\Delta T_{s,k} = \left(z_k^n - T_{b,k}^n\right) - \left(z_k^{n+1} - T_{b,k}^{n+1}\right). \quad (4)$$

Here z represents the channel bed elevation, the measured values of which were used in the computations of the bed material composition. Since the volume of each fraction in the corresponding substrate layer is also known, the new composition of active bed layer can easily be determined as the computations are done for the next time interval.

4.3. Effect of Clay Content on Bed Load Transport

[30] The erosion and transport rate of cohesionless uniform and nonuniform sediments can be determined with sufficient accuracy by using any of the various methods available for its computation [*Garde and Ranga Raju*, 2006] by using the knowledge on grain density, size and gradation, and flow and fluid parameters. To quantify the transport rates of cohesive sediments during the erosion in comparison with those of cohesionless sediments of similar bulk characteristics, the percentage of clay and other size fractions in the bed material was computed first by using the formulations for the ABL (namely, equations (1)–(4)). The percentages of clay and other size fractions were computed at those time periods when the observations for flow and bed profiles were also made. Using the computed friction slope from observed water surface profile at these time intervals, the grain shear stress was computed which corresponded to the simultaneously measured transport rate.

[31] The bed load transport rate of the cohesionless sediment, by weight per unit width of the channel $q_{B,i}$, can be computed from the dimensionless bed load parameter ($\phi_{B,i}$), and for nonuniform sediment it can be expressed as [*Garde and Ranga Raju*, 2006]

$$\phi_{B,i} = \frac{i_B q_{B,i}}{i_b \gamma_s}\sqrt{\frac{\gamma_f}{\Delta\gamma_s g d_i^3}}, \quad (5)$$

where $q_{B,i}$ is the fraction-wise bed load transport rate by weight per unit width of channel and $\Delta\gamma_s = \gamma_s - \gamma_w$, with γ_s being specific weight of the sediment and γ_w being specific weight of the water; i_B and i_b are the fraction of the size d_i in the bed load and the bed material, respectively; and d_i is the fraction size. The two sizes, gravel (d_g) and sand (d_s), were considered for the computation of fraction-wise bed load transport in the presence of cohesion.

[32] As per *Patel and Ranga Raju* [1996], for nonuniform cohesionless bed material

$$\phi_{B,i} = f\left(\frac{\tau_o'}{\Delta\gamma_s d_i}, \xi_{B,i}\right). \quad (6)$$

In above, τ_o' is grain shear stress which can be calculated as per *Misri et al.* [1984], and $\xi_{B,i}$ is the exposure-sheltering coefficient for different sizes in the sediment mixture. The *Patel and Ranga Raju* [1996] method is used to compute the values of $\xi_{B,i}$ for different size fractions of the cohesionless component of the cohesive sediment mixture in the present study. The dimensionless grain shear stress $\tau_{*,i}'$ for the cohesionless sediment size fraction d_i is defined as

$$\tau_{*,i}' = \left(\frac{\tau_o'}{\Delta\gamma_s d_i}\right). \quad (7)$$

Figures 7, 8, and 9 are prepared using the present data which depict the variation of observed $\phi_{B,i}$ (representing the observed transport rates of the cohesionless sediment size fractions) with computed values of $\xi_{B,i}\tau_{*,i}'$ for various percentages of clay present in the bed material mixture. Figures 7, 8, and 9 were made by following the procedure of

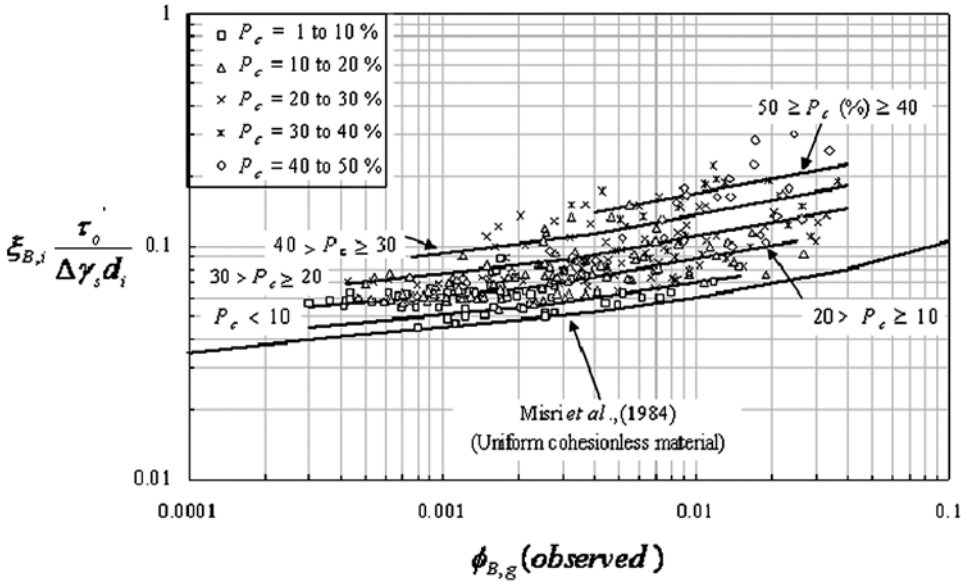

Figure 7. Variation of transport rate of gravel with grain shear stress for clay-gravel mixtures.

plotting followed by *Einstein* [1950] for study of the transport rates of different size fractions in a cohesionless sediment mixture. Note that $\phi_{B,i} = \phi_{B,g}$ for gravel size fraction while $\phi_{B,i} = \phi_{B,s}$ for sand size fraction of the corresponding bed material mixture. In Figures 7–9, P_c is the percentage of clay present in the bed material. For the given value of $\xi_{B,i}\tau^{'}_{*,i}$ the value of transport parameter $\phi_{B,i}$ is seen to be much smaller for the cohesionless size fractions of the cohesive sediment mixture compared with this value for same size fractions in a cohesionless sediment mixture. Figures 7–9 indeed reveal that transport rates of the cohesionless sediment size fractions become drastically different due to the presence of clay in the bed material, but a systematic variation of the transport rates with clay content present among the mentioned data may be noted in Figures 7–9. The parallel lines in Figures 7–9 were drawn by eye judgment and merely illustrate the fact that the data can be very well partitioned based on the values of P_c. It is important to note, however, that the experiments and hence determination of bed shear stress were done under the dynamic process of entrainment, deposition, and transport. The bed shear stress gets altered as soon as erosion starts because of nonuniform erosion pattern and also due to cohesive sediment in suspension which may cause drag reduction. The large scatter of data as depicted in Figures 7–9 is therefore attributed to these uncertainties.

[33] The data on transport rates caused by erosion of the mentioned size fractions in the mixtures not containing clay, however, were noticed to perfectly follow the method of *Patel and Ranga Raju* [1996] for nonuniform cohesionless

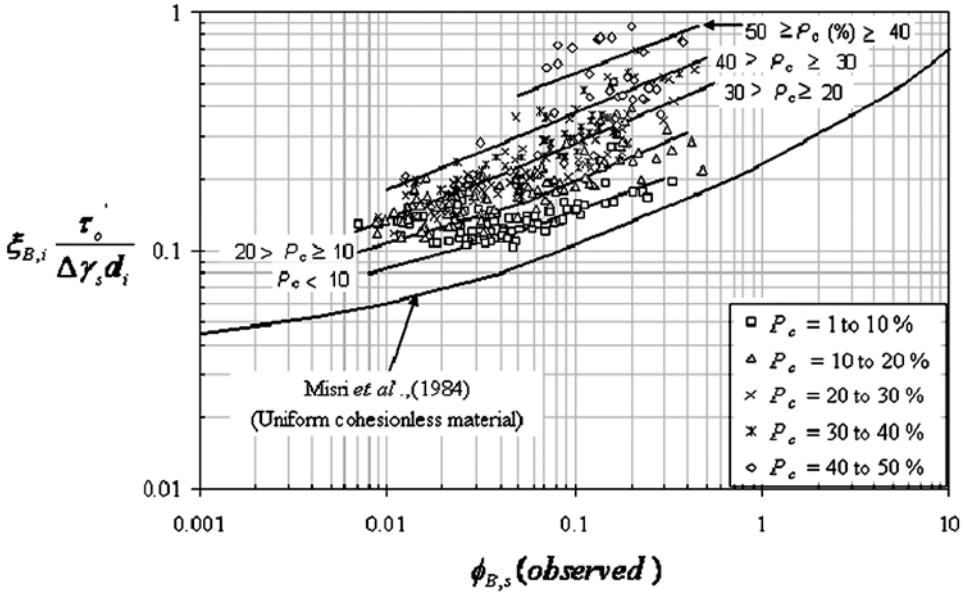

Figure 8. Variation of transport rate of sand with grain shear stress for clay-sand-gravel mixtures.

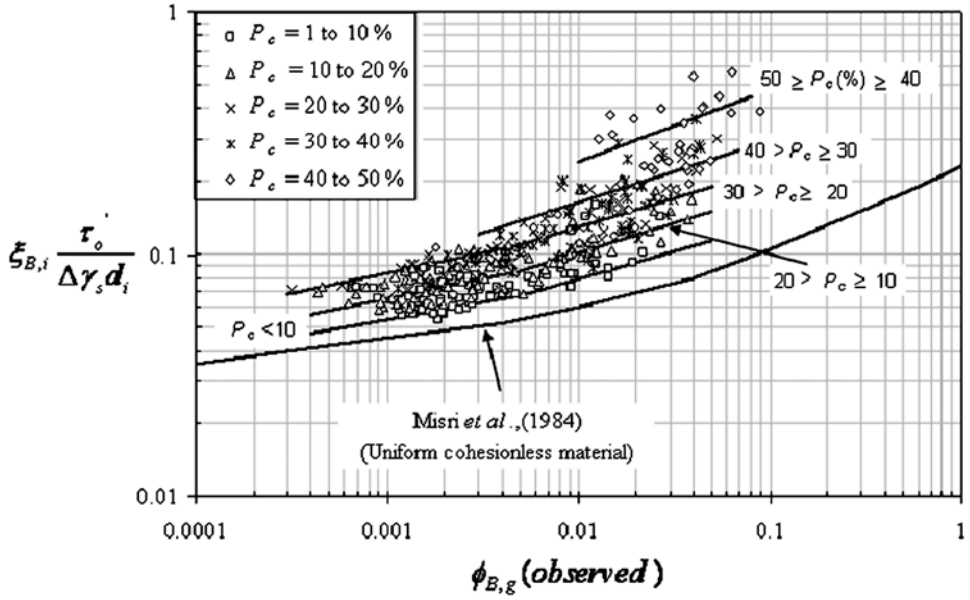

Figure 9. Variation of transport rate of gravel with grain shear stress for clay-sand-gravel mixtures.

sediments, whereas the relationship of *Misri et al.* [1984] was found to well estimate the transport rates caused by erosion of the uniform size cohesionless sediment in the absence of clay [*Jain*, 2008].

[34] The unconfined compressive strength of sediment bed at any particular time of experimental run is denoted as UCS', and this was defined as

$$\mathrm{UCS}' = \left(\frac{P_c}{P_{co}}\right)\mathrm{UCS}. \tag{8}$$

Here P_{co} is the initial percentage of clay (prior to the occurrence of erosion) in the bed material. $P_{co} = P_c$ for the initial observation of each experimental run. To quantify the effect of shear strength of cohesive sediments on the transport rates, the variation of UCS′ with the corresponding observed transport rate is studied. Figure 10 was prepared in which the data were partitioned according to three ranges of UCS' values. It was noticed that the erosion rate decreases with an increase in UCS' values of the cohesive sediments. The ability of the cohesive sediment to resist erosion increases with the increase in unconfined compressive strength of sediment mixtures is well depicted by Figure 10. Such results have also been reported earlier by *Kamphuis and Hall* [1983] in the context of erosion of clay-sand mixtures, and similarly *Robinson and Hanson* [1995] observed the head-cut advance rate to decrease with an increase in the UCS' values of the cohesive sediment consisting of clay-silt-sand mixtures. The zones on different UCS' values are depicted by dotted lines (drawn by eye

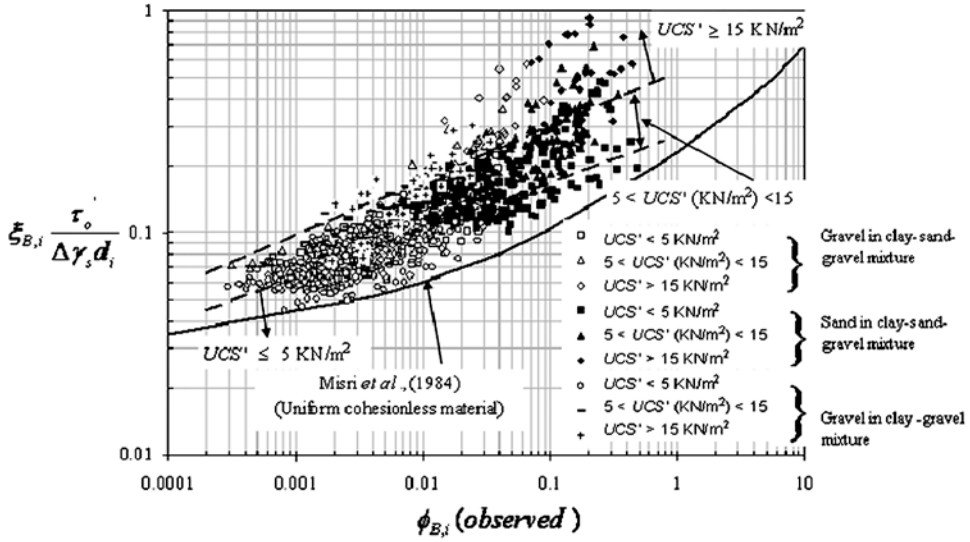

Figure 10. Variation of transport rate with UCS' for clay-gravel mixtures and clay-sand-gravel mixtures.

judgment) in Figure 10 as a few data encroached in to the neighboring zones, while P_c and flow shear stress were high.

5. Dimensional Analysis

[35] An examination of the various analytical and semi-theoretical approaches on bed load transport of cohesionless sediments revealed that the transport rate in the case of cohesionless sediments is a function of grain shear stress and particle size only [*Garde and Ranga Raju*, 2006]. However, in the case of cohesive sediments, because of the physicochemical properties, other variables such as clay percentage, dry density, unconfined compression strength, etc., also become important in the transport during the process of erosion as they represent the electrochemical forces prevalent in this process. Keeping these in view, the following functional form of relationship is written in terms of the easily measurable variables, for the computation of transport rate during the erosion in case of cohesive sediments:

$$q_{Bc,i} = f\left(q_{B,i}, P_c, d_a, C_u, \phi_c, \phi_{sh}, \gamma_d, \gamma_w, \Delta\gamma_s, \mathrm{UCS}'\right). \quad (9)$$

Here $q_{Bc,i}$ is the bed load transport rate of given size fraction present in cohesive sediment bed; $q_{B,i}$ is the bed load transport rate of same size fraction in cohesionless sediment bed under the same flow conditions; C_u and ϕ_c are the cohesion and the angle of internal friction, respectively, for clay at optimum moisture content; ϕ_{sh} is the angle of repose/internal friction of cohesionless sediment for the respective sediments present in the mixture; γ_d is the dry density of cohesive sediment mixture; γ_w is specific weight of water, $\Delta\gamma_s$ is submerged specific weight; and d_a is the arithmetic mean size of the bed material mixture. The parameters P_c, C_u, ϕ_c, ϕ_s, $\Delta\gamma_s$, and d_a can be expressed into dimensionless form as below [*Ansari et al.*, 2002]:

$$C_* = \frac{P_c C_u}{\Delta\gamma_s d_a} \quad (10)$$

$$\phi_* = \frac{P_c \tan\phi_c + (1 - P_c)\tan\phi_{sh}}{\tan\phi_{sh}}. \quad (11)$$

The variable UCS' can also be written in the dimensionless form as

$$\mathrm{UCS}^* = \frac{\mathrm{UCS}'}{\Delta\gamma_s d_a}. \quad (12)$$

It is necessary to mention here that for the cohesive sediments which are formed by mixture of clay, silt, sand and gravel, the term C_* and ϕ_* are improved indicators of their cohesiveness since values of C_* and ϕ_* are derived by giving weight to C_u and ϕ_c according to the percentage of clay content available in the sediment mixture. Likewise the term *UCS** appropriately simulates the strength parameter of the cohesive sediment mixture. It also represents engineering (mechanical) behavior of the cohesive sediments originating from different hydrogeological regions and therefore having varying physicochemical characteristics [*Kothyari and Jain*, 2008]. The parameter UCS* is also considered to account for the scaling effects related to the behavior of clay material. On the basis of the above, equation (9) reduces to

$$q_{Bc,i} = f\left(q_{B,i}, C_*, \phi_*, \gamma_d, \gamma_w, \mathrm{UCS}^*\right). \quad (13)$$

The variables of equation (9) can also be easily merged into the following nondimensional groups:

$$\frac{q_{Bc,i}}{q_{B,i}} = f\left(\frac{C_*}{\phi_*}, \mathrm{UCS}^*, \frac{\gamma_d}{\gamma_w}\right). \quad (14)$$

The range of variable γ_d/γ_w covered by the present data was from 1.54 to 2.12. The analysis of data indicated that variation in γ_d/γ_w within this small range could not fully explain the variations in $q_{Bc,i}/q_{B,i}$, and therefore the variable γ_d/γ_w has been dropped from the further analysis and new functional relationship for q_{Bc} is written as

$$\frac{q_{Bc,i}}{q_{B,i}} = f\left(\left(1 + \frac{C_*}{\phi_*}\right), (1 + \mathrm{UCS}^*)\right). \quad (15)$$

It is worthwhile to use the variable $(1 + (C_*/\phi_*))$ instead of C_*/ϕ_* so that $q_{Bc,i} = q_{B,i}$, while $P_c = 0$. With similar consideration the variable (1 + UCS*) is used instead of UCS* to account for both the hard consistencies and the soft consistencies of cohesive sediments [*Kothyari and Jain*, 2008]. The functional relationship can be used to develop a method to compute the transport rate of different size fractions in a sediment mixtures having cohesion. The value of $q_{B,i}$ to be used in equation (15) can be determined by using an appropriate relationship for the transport of the cohesionless sediment. In the present study, the relationship of *Patel and Ranga Raju* [1996] is used for this purpose in the case of nonuniform cohesionless sediment.

[36] This is important to note again that an appreciable difference was observed between the process of erosion and transport of cohesionless and cohesive sediments (Figures 7–9). However, no previous data are available for the study of transport rate by the erosion process of clay-gravel and clay-sand-gravel mixtures whereas such sediment mixtures are noticed to occur under different conditions in nature. Analysis of the presently collected data revealed that $q_{Bc,i}/q_{B,i}$ is inversely proportional to $(1 + (C_*/\phi_*))$ for both the sediment mixtures as shown in Figures 11 and 12. Analysis also revealed that $q_{Bc,i}/q_{B,i}$ is inversely proportional to (1 + UCS*) for both the sediment mixtures as shown in Figure 13. The observations corresponding to zero value of UCS, however, are not shown in Figure 13.

6. Results and Discussions

[37] After making a number of trials by using all the relevant dimensionless parameters, it was found that a satisfactory relationship could be derived for the variation of $q_{Bc,i}/q_{B,i}$ with change in values of $(1 + (C_*/\phi_*))$ and (1 + UCS*) as shown in Figure 14 for the transport of gravel in clay-gravel mixture and transport of sand and gravel in clay-sand-gravel mixtures.

[38] The following expressions are proposed for describing Figure 14 to compute bed load transport of gravel and

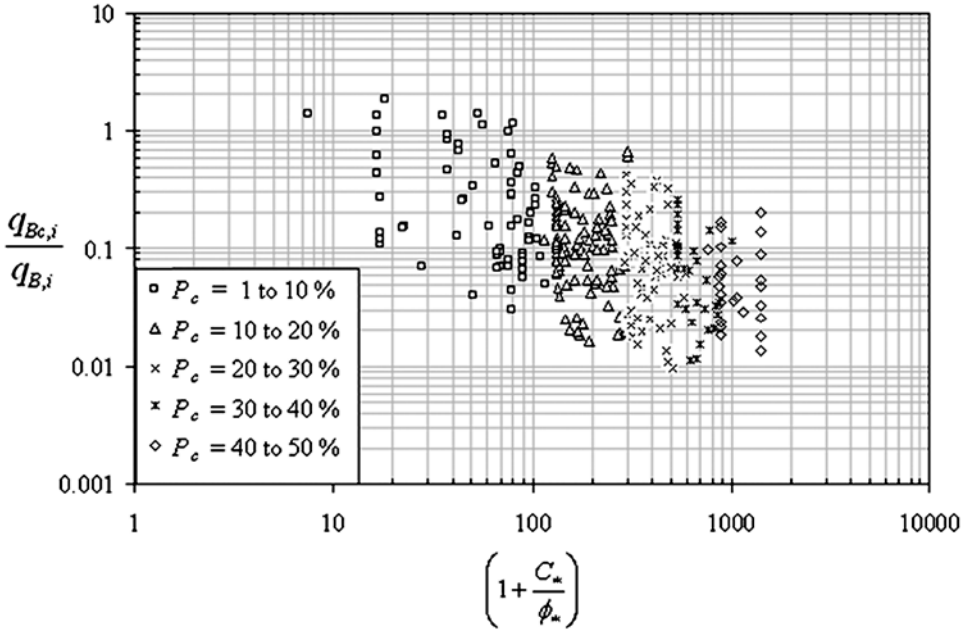

Figure 11. Variation of $q_{Bc,i}/q_{B,i}$ with $(1 + C_*/\phi_*)$ for gravel transport rate in case of clay-gravel mixtures.

sand in case of cohesive sediment consisting of clay-sand-gravel and clay-gravel mixtures after applying suitable correction for the presence of cohesive material, i.e., clay:

For $0.02 < (\xi_{B,i}\tau'_{*,i}) < 0.062$

$$\phi_{B,i} = 10^8\left(\xi_{B,i}\tau'_{*,i}\right)^{8.345} * \left(1+\frac{C_*}{\phi_*}\right)^{(-8/25)}\left(1+\mathrm{UCS}^*\right)^{(-1/5)} \tag{16}$$

For $0.062 < (\xi_{B,i}\tau'_{*,i}) < 0.175$

$$\phi_{B,i} = \left[-2545.5\left(\xi_{B,i}\tau'_{*,i}\right)^5 - 412.23\left(\xi_{B,i}\tau'_{*,i}\right)^4 + 518.81\left(\xi_{B,i}\tau'_{*,i}\right)^3 - 81.01\left(\xi_{B,i}\tau'_{*,i}\right)^2 + 6.19\left(\xi_{B,i}\tau'_{*,i}\right) - 0.178\right] * \left(1+\frac{C_*}{\phi_*}\right)^{(-8/25)}\left(1+\mathrm{UCS}^*\right)^{(-1/5)} \tag{17}$$

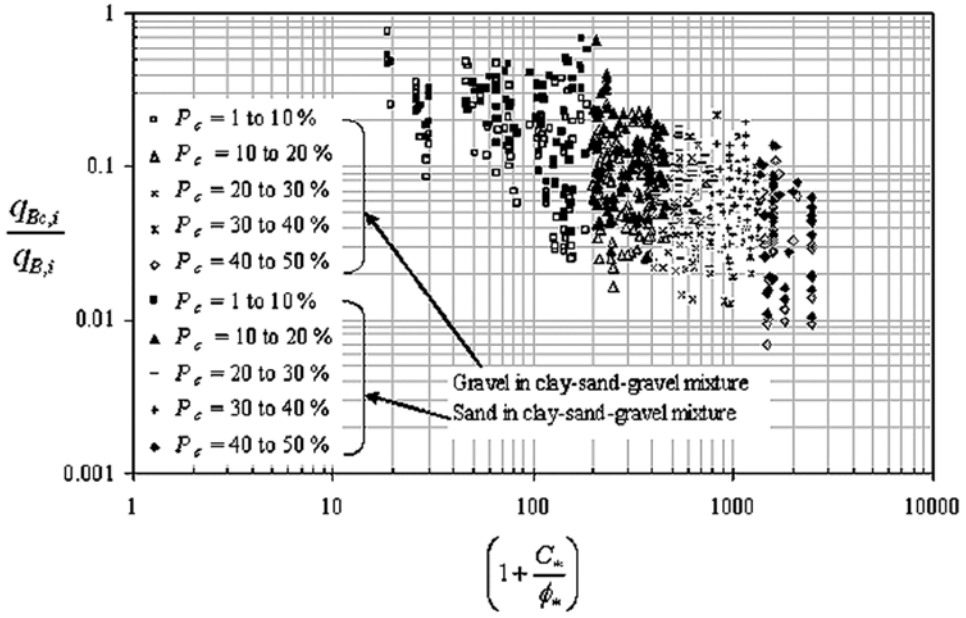

Figure 12. Variation of $q_{Bc,i}/q_{B,i}$ with $(1 + C_*/\phi_*)$ for sand and gravel transport rate in case of clay-sand-gravel mixtures.

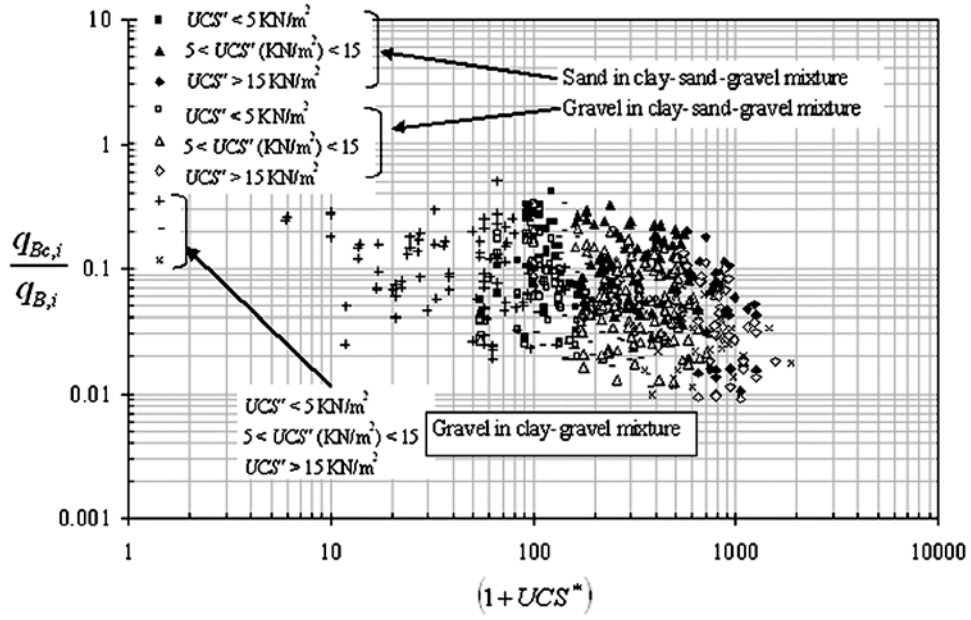

Figure 13. Variation of $q_{Bc,i}/q_{B,i}$ with (1 + UCS*) for transport rate of sand and gravel in case of clay-gravel mixtures and clay-sand-gravel mixtures.

For $0.175 < (\xi_{B,i}\tau'_{*,i}) < 1.83$

$$\phi_{B,i} = \left[13.895\left(\xi_{B,i}\tau'_{*,i}\right)^{1.9356}\right] * \left(1+\frac{C_*}{\phi_*}\right)^{(-8/25)}\left(1+\mathrm{UCS}^*\right)^{(-1/5)}. \quad (18)$$

During erosion and transport of sediment mixtures, the finer particles of the mixture are sheltered by the coarser particles. The finer particles of a sediment mixture therefore are subjected to smaller drag by flow compared with the drag these particles would face by same flow, if these exist in a uniform sediment bed. Similarly, the coarser-sized particles of sediment mixture are subjected to larger drag due to the exposure effect. The factor $\xi_{B,i}$ defined by *Patel and Ranga Raju* [1996] amply simulates, albeit empirically, the exposure-sheltering effects in transport of sediment mixtures. The effects on bed load transport of varying proportions of clay in the sediment mixture and the strength of cohesive sediment bed (represented by the parameter UCS) are, however, quantified by equations (16)–(18), albeit empirically. In these equations, negative exponents of the parameters representing cohesion of sediment bed are

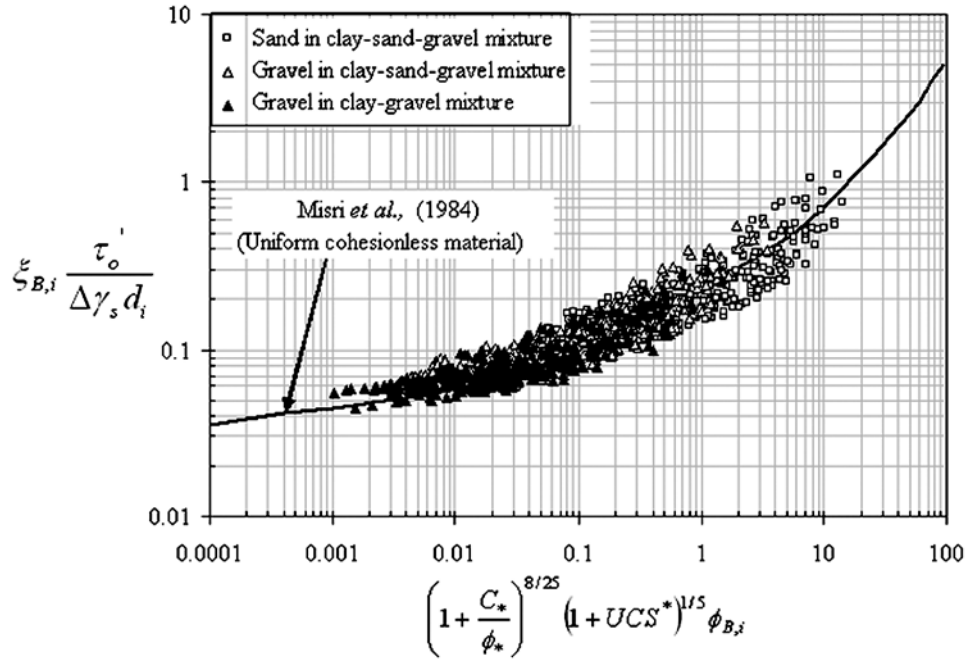

Figure 14. Variation of transport parameter with grain shear stress for clay-gravel and clay-sand-gravel mixtures.

Table 3. Summary of Comparison Between Computed and Observed Value of Bed Load Transport Rate

		Discrepancy Ratio					
			Percent of Data in Range				
Cohesive Sediments	Material	Mean ($\bar{R}$)	0.75–1.25	0.5–2.0	0.33–3.0	Standard Deviation (σ)	Number of Data Sets (N)
Clay-gravel mixtures	gravel	1.415	21.47	58.97	83.65	1.09	312
Clay-sand-gravel mixtures	gravel	1.715	24.08	56.09	84.98	1.352	353
	sand	1.084	24.36	62.89	85.83	0.771	353

theoretically logical as a reduction occurs in the rate of bed load transport due to cohesion. Indeed Figures 4–6 depicted this process whereas equations (16)–(18) are able to quantify the same.

[39] For testing the goodness of fit of the proposed relations, the discrepancy ratio and standard deviation [*Yang et al.*, 1996] are used as described below.

Discrepancy ratio

$$R_i = \frac{q_{Bcoi}}{q_{Boi}}. \tag{19}$$

Here q_{Bcoi} and q_{Boi} are corresponding rates of computed and observed bed load transport respectively.

Mean discrepancy ratio

$$\bar{R} = \frac{\sum R_i}{N}. \tag{20}$$

Here N is total number of data used for the comparison.

Standard deviation

$$\sigma = \sqrt{\frac{\sum (R_i - \bar{R})^2}{N-1}}. \tag{21}$$

Comparisons between computed and observed bed load transport rate based on discrepancy ratio and standard deviation are summarized in Table 3.

[40] The goodness of fit of the proposed equations is also measured on the difference between computed and observed results using the following parameters [*Yang et al.*, 1996]:

$$\bar{R}_d = \frac{\sum [(q_{Bcoi} - q_{Boi})/q_{Boi}]}{N} \tag{22}$$

$$\sigma_d = \sqrt{\frac{\sum (q_{Bcoi} - q_{Boi})^2}{N-1}}. \tag{23}$$

For a perfect fit, $\bar{R}_d = 0$ and $\sigma_d = 0$.

[41] In addition, the goodness of fit of the proposed equations is also measured by calculating average discrepancy ratio and standard deviation based on the average value of the logarithm ratio between computed and observed results using the following parameters [*Yang et al.*, 1996]:

$$D_i = \log q_{Bcoi} - \log q_{Boi} \tag{24}$$

$$\bar{D}_a = \frac{\sum D_i}{N} \tag{25}$$

$$\sigma_a = \sqrt{\frac{(D_i - \bar{D}_a)^2}{N-1}}. \tag{26}$$

For a perfect fit, $\bar{D}_a = 0$ and $\sigma_a = 0$.

[42] The comparisons between computed and observed bed load transport rate based on the average logarithm ratio and the difference between computed and observed results are summarized in Table 4, which indicates that the accuracy of sediment transport predictions for cohesive sediments are similar to those of the *Yang et al.* [1996] and *Almedeij and Diplas* [2003] relationships for the cohesionless sediment.

[43] The procedure for computation of $q_{Bc,i}$ is as follows:

[44] 1. Making use of the known percentage of various fractions in bed material prior to the occurrence of flow and transport, compute the percentages of various size fractions by using active bed layer formulation, namely, equations (1)–(4) at the times when transport rate is needed to be estimated.

[45] 2. Determine the value of arithmetic mean size, d_a, of the bed material and compute C_*, ϕ_*, UCS* using equations (10), (11), and (12), respectively.

[46] 3. Compute $\xi_{B,i}$ ($\tau'_o/\Delta\gamma_s d_i$) as per *Patel and Ranga Raju* [1996] for cohesionless nonuniform sediment mixtures.

[47] 4. Compute the value of $\phi_{B,i}$ from bed load transport law as per Figure 14 or using equations (16)–(18) as per the prevailing condition.

[48] 5. Compute the bed load transport rate $q_{Bc,i}$ as per the following equation for cohesive nonuniform sediment:

$$q_{Bc,i} = \phi_{B,i}\, i_b\, \gamma_s \sqrt{\frac{\Delta\, \gamma_s\, g\, d_i^3}{\gamma_f}}. \tag{27}$$

The observed values of bed load transport rate of gravel and sand sizes present in the cohesive sediment mixtures are

Table 4. Summary of Comparison Between Computed and Observed Value of Bed Load Transport Rate Based on Logarithm Ratio and Difference Between Computed and Measured Values

Cohesive Sediments	Material	$\bar{D}_a$	σ_a	$\bar{R}_d$	σ_d	Number of Data Sets
Clay-gravel mixtures	gravel	0.0265	0.335	0.415	0.065	312
Clay-sand-gravel mixtures	gravel	0.113	0.328	−0.0128	0.0755	353
	sand	−0.0703	0.308	0.0839	0.008	353

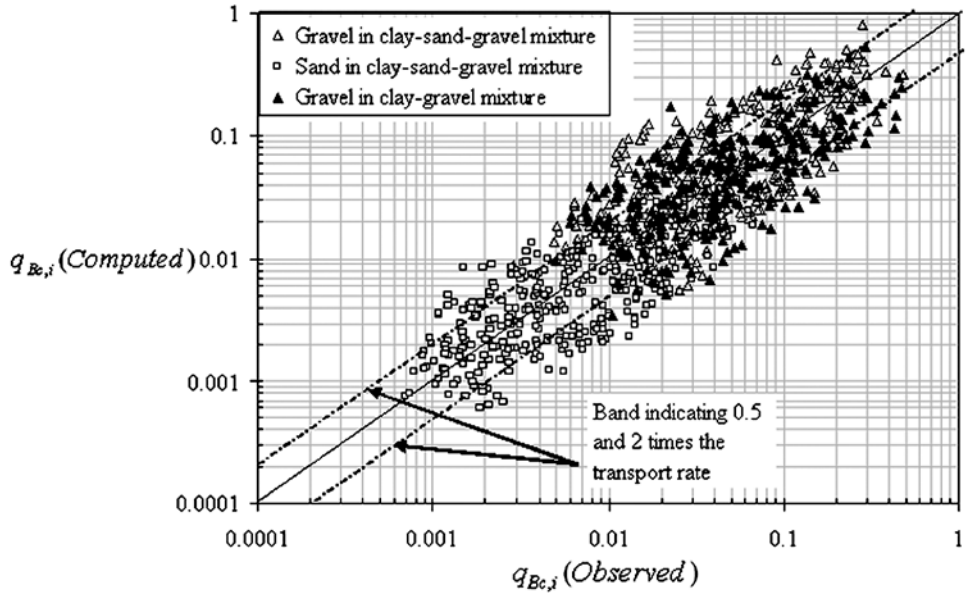

Figure 15. Observed versus computed bed load transport rate of sand and gravel for clay-gravel and clay-sand-gravel mixtures.

plotted against their corresponding values computed by the proposed method as shown in Figure 15. It can be seen from Figure 15 that, in general, the proposed method produced results with a maximum error of about twofold and threefold for about 80 to 90% of the total data. The scatter of the results by the proposed method as seen in Figure 15 albeit is large, but is acceptable in the context of similar results generally reported in the literature on transport studies of the cohesionless sediment mixtures [*Yang et al.*, 1996; *Almedeij and Diplas*, 2003].

[49] As already mentioned, the measurements on sediment transport are taken under the dynamic process of entrainment, deposition, and transport. The bed shear stress gets altered as soon as erosion starts because of nonuniform erosion pattern and also due to cohesive sediment in suspension which may cause drag reduction. Also the erosion and transport occurs due to fluctuations of the velocity from its mean. Consequently, observed sediment load transport rate over a time period can be significantly higher or lower than computed transport rate [*Garde and Ranga Raju*, 2006]. Scattering of the data as depicted in Figure 15 is attributable to this phenomenon and to the uncertainties associated with the measurements.

[50] It is significant to note in the above, however, that in the absence of cohesion, the proposed relations for bed load transport rate reduce to the transport rate of cohesionless sediments for the given flow condition. Several other dimensionless groups also were used to study the variations in $q_{Bc,i}/q_{B,i}$. Only the best results obtained, however, are reported above.

7. Conclusions

[51] Numerous experiments were conducted to study the bed load transport rate resulting from the erosion of cohesive sediments made up of clay mixed in varying proportions with uniform and nonuniform cohesionless sediments. Two types of sediment mixtures were used: (1) clay mixed in proportions varying from 10% to 50% with fine gravel and (2) clay mixed in proportions varying from 10% to 50% with sand and fine gravel of equal proportions. The erosion characteristics and the transport rate are noticed (Figures 4–9) to be significantly affected by the proportion of clay present in the mixture. Depending upon the clay percentage available in the bed material and applied shear stress by the flow, the processes representing rill and gully erosion have been observed to occur during the erosion and transport of cohesive sediment mixtures.

[52] On the basis of dimensional considerations a functional relationship for the determination of bed load transport rates of sand and gravel present in the sediment mixtures having cohesion were derived. Equations (16)–(18) are proposed for the estimation of transport rate of gravel occurring by the erosion of clay-gravel mixtures and for the estimation of transport rates of gravel and sand occurring by the erosion of the clay-sand-gravel mixture. The significant reduction that occurs in the bed load transport rate of cohesionless material in the presence of clay in the mixture is amply reflected by these relations. In the absence of cohesion, the proposed method reduces to the *Patel and Ranga Raju* [1996] method for the estimation of bed load transport of nonuniform cohesionless sediments under the varying flow conditions.

Notation

ABL active bed layer.
B flume width ($M^0\ L^1\ T^0$).
C_u cohesion at optimum moisture content ($M^1\ L^{-1}\ T^{-2}$).
C_* dimensionless clay content defined as $P_c C_u/\Delta\gamma_s d_a$ ($M^0\ L^0\ T^0$).
Ca calcium.
d_{50} sediment size such that 50% of the bed material is finer than this by weight ($M^0\ L^1\ T^0$).
e void ratio ($M^0\ L^0\ T^0$).

d_a arithmetic mean size ($M^0\ L^1\ T^0$).
h flow depth ($M^0\ L^1\ T^0$).
Na sodium.
P_c clay percentage in the bed material at the time of measurement of the transport rate.
P_{co} initial percentage of clay in the sediment bed ($M^0\ L^0\ T^0$).
q_{Bcoi} computed value of bed load transport by erosion ($M^1\ L^0\ T^{-3}$).
q_{Boi} observed value of bed load transport by erosion ($M^1\ L^0\ T^{-3}$).
q_{Bg} bed load transport of gravel ($M^1\ L^0\ T^{-3}$).
q_{Bs} bed load transport of sand ($M^1\ L^0\ T^{-3}$).
Q_b volumetric rate of bed load discharge ($M^0\ L^3\ T^{-1}$).
Q_s volumetric rate of suspended load discharge ($M^0\ L^3\ T^{-1}$).
R_i discrepancy ratio ($M^0\ L^0\ T^0$).
$\bar{R}$ average discrepancy ratio ($M^0\ L^0\ T^0$).
$\bar{R}_d$ average discrepancy ratio based on the difference of computed and observed value.
S_f energy slope ($M^0\ L^0\ T^0$).
T_b thickness of active bed layer ($M^0\ L^1\ T^0$).
U mean velocity of flow ($M^0\ L^1\ T^{-1}$).
UCS unconfined compressive strength of cohesive sediments ($M^1\ L^{-1}\ T^{-2}$).
V volume of sediment in modified ABL ($M^0\ L^3\ T^0$).
W antecedent moisture content ($M^0\ L^0\ T^0$).
γ_d dry density of sediment bed ($M^1\ L^{-2}\ T^{-2}$).
γ_s specific weight of sediment ($M^1\ L^{-2}\ T^{-2}$).
γ_w specific weight of water ($M^1\ L^{-2}\ T^{-2}$).
$\Delta\gamma_s$ submerged specific weight ($M^1\ L^{-2}\ T^{-2}$).
τ_o' grain shear stress ($M^1\ L^{-1}\ T^{-2}$).
τ_*' dimensionless grain shear stress of cohesionless sediments ($M^0\ L^0\ T^0$).
τ_{oc} critical shear stress of the arithmetic mean size ($M^1\ L^{-1}\ T^{-2}$).
τ_o average shear stress of flow ($M^1\ L^{-1}\ T^{-2}$).
Δx computational spatial step ($M^0\ L^1\ T^0$).
Δt computational time step ($M^0\ L^0\ T^1$).
σ standard deviation of the computed result ($M^0\ L^0\ T^0$).
σ_a standard deviation of the computed results based on logarithm ratio ($M^0\ L^0\ T^0$).
σ_d standard deviation the computed results based on difference ($M^0\ L^0\ T^0$).
$\phi_{B,i}$ dimensionless bed load transport parameter for sediment size d_i ($M^0\ L^0\ T^0$).
ϕ_c angle of repose or internal friction for cohesive sediment ($M^0\ L^0\ T^0$).
ϕ_{Bg} dimensionless bed load transport parameter for gravel transport ($M^0\ L^0\ T^0$).
ϕ_{Bs} dimensionless bed load transport parameter for sand transport ($M^0\ L^0\ T^0$).
ϕ_{sh} angle of repose or internal friction for cohesionless sediment ($M^0\ L^0\ T^0$).
λ porosity of sediment bed material ($M^0\ L^0\ T^0$).
$\xi_{B,i}$ exposure-sheltering coefficient for sediment size d_i ($M^0\ L^0\ T^0$).

[53] **Acknowledgments.** The authors wish to sincerely thank Gordon Grant and other members of the editorial team of *WRR* whose comments have resulted in an improvement in the quality of this paper.

References

Aberle, J., V. Nikora, and R. Walters (2004), Effect of bed material properties on cohesive sediment erosion, *J. Mar. Geol.*, *207*, 83–93, doi:10.1016/j.margeo.2004.03.012.

Aberle, J., V. Nikora, and R. Walters (2006), Data interpretation for in-situ measurement of cohesive sediment erosion, *J. Hydraul. Eng.*, *132*(6), 581–588, doi:10.1061/(ASCE)0733-9429(2006)132:6(581).

Abt, S. R., and J. F. Ruff (1982), Estimating culvert scour in cohesive material, *J. Hydraul. Eng.*, *108*(1), 25–34.

Almedeij, J. H., and P. Diplas (2003), Bed load transport in gravel-bed streams with unimodal sediment, *J. Hydraul. Eng.*, *129*(11), 896–904, doi:10.1061/(ASCE)0733-9429(2003)129:11(896).

Amos, C. L., T. Feeney, T. F. Sutherland, and J. L. Luternauer (1997), The stability of fine grained sediments from the Fraser River delta, *Estuarine Coastal Shelf Sci.*, *45*, 507–524, doi:10.1006/ecss.1996.0193.

Ansari, S. A., U. C. Kothyari, and K. G. Ranga Raju (2002), Influence of cohesion on scour around bridge piers, *J. Hydraul. Res.*, *40*(6), 717–729.

Ansari, S. A., U. C. Kothyari, and K. G. Ranga Raju (2003), Influence of cohesion on scour under submerged circular vertical jet, *J. Hydraul. Eng.*, *129*(12), 1014–1019, doi:10.1061/(ASCE)0733-9429(2003)129:12(1014).

Arulanandan, K. E. (1975), Fundamental aspect of erosion of cohesive soils, *J. Hydraul. Div. Am. Soc. Civ. Eng.*, *101*(HY5), 635–639.

Borah, D. K., C. V. Alonso, and S. N. Prasad (1982), Routing graded sediments in stream formulations, *J. Hydraul. Div. Am. Soc. Civ. Eng.*, *108*(12), 1486–1503.

Briaud, J. F., C. K. F. Ting, H. C. Chen, G. Rao, S. Perugu, and G. Wei (1999), SRICOS: Prediction of scour rate in cohesive soils at bridge piers, *J. Geotech. Geoenviron. Eng.*, *125*(4), 237–246, doi:10.1061/(ASCE)1090-0241(1999)125:4(237).

Briaud, J. F., C. K. F. Ting, H. C. Chen, Y. Cao, S. W. Han, and K. W. Kwak (2001), Erosion function apparatus for scour rate predictions, *J. Geotech. Geoenviron. Eng.*, *127*(2), 105–113, doi:10.1061/(ASCE)1090-0241(2001)127:2(105).

Bureau of Indian Standards (BIS) (1975), Determination of in-place density by core-cutter method, *IS 2720*, part XXIX, New Delhi.

Bureau of Indian Standards (BIS) (1991), Determination of shear strength by unconfined compression method, *IS 2720*, part X, New Delhi.

Correia, L. R. P., B. G. Krishnappan, and W. H. Graf (1992), Fully coupled unsteady mobile boundary flow model, *J. Hydraul. Eng.*, *118*(3), 476–494, doi:10.1061/(ASCE)0733-9429(1992)118:3(476).

Dey, S., and B. Westrich (2003), Hydraulics of submerged jet subject to change in cohesive bed geometry, *J. Hydraul. Eng.*, *129*(1), 44–53, doi:10.1061/(ASCE)0733-9429(2003)129:1(44).

Einstein, H. A. (1950), The bed load function for sediment transportation in open channel flows, *Tech. Bull. 1026*, U.S. Dep. of Agric., Washington, D. C.

Garde, R. J., and K. G. Ranga Raju (2006), *Mechanics of Sediment Transport and Alluvial Stream Problems*, 3rd ed., New Age Int. Publ., New Delhi.

Grissinger, E. H. (1966), Resistance of selected clay systems to erosion by water, *Water Resour. Res.*, *1*, 131–139, doi:10.1029/WR002i001p00131.

Grissinger, E. H., W. C. Little, and J. B. Murphey (1981), Erodibility of stream bank materials of low cohesion, *Trans. ASAE*, *24*(3), 624–630.

Hanson, G. J. (1990), Surface erodibility of earthen channels at high stress: Part I. Open channel testing, *Trans. ASAE*, *33*(1), 127–131.

Hanson, G. J., and S. L. Hunt (2006), Determining the erodibility of compacted soils for embankment dams, in *Proceeding of USSD Conference*, pp. 311–320, U.S. Soc. on Dams, Denver, Colo.

Hanson, G. J., and K. M. Robinson (1993), Influence of soil moisture and compaction on spillway erosion, *Trans. ASAE*, *36*(5), 1349–1352.

Houwing, E. J. (1999), Determination of the critical erosion threshold of cohesive sediments on itertidal mudflats along the Dutch Wadden Sea coast, *Estuarine Coastal Shelf Sci.*, *49*, 545–555, doi:10.1006/ecss.1999.0518.

Jain, R. K. (2008), Influence of cohesion on detachment and transport of clay-sand-gravel mixtures, Ph.D. thesis, 245 pp., Dep. of Civ. Eng., Indian Inst. of Technol., Roorkee, India.

Jepsen, R., J. Roberts, and W. Lick (1997), Effect of sediment bulk density on erosion rates, *Water Air Soil Pollut.*, *99*, 21–37.

Kamphuis, J. W., and K. R. Hall (1983), Cohesive material erosion by unidirectional current, *J. Hydraul. Div. Am. Soc. Civ. Eng.*, *109*(1), 39–62.

Karim, M. F., and J. F. Kennedy (1982), IALLUVIAL: A computer based flow and sediment routing model for alluvial stream and its application to Missouri River, *IIHR Rep. 250*, Univ. of Iowa, Iowa city.

Kothyari, U. C., and R. K. Jain (2008), Influence of cohesion on incipient motion condition of sediment mixtures, *Water Resour. Res.*, *44*, W04410, doi:10.1029/2007WR006326.

Kothyari, U. C., A. K. Tiwari, and R. Singh (1997), Estimation of temporal variation of sediment yield from small catchments through the kinematic method, *J. Hydrol.*, *203*(1), 39–57, doi:10.1016/S0022-1694(97)00084-X.

Kuti, E. O., and C. Yen (1976), Scouring of cohesive soils, *J. Hydraul. Res.*, *14*, 195–206.

Mazurek, K. A., N. Rajaratnam, and D. C. Sego (2001), Scour of cohesive soil by submerged circular turbulent impinging jets, *J. Hydraul. Eng.*, *127*(7), 598–606, doi:10.1061/(ASCE)0733-9429(2001)127:7(598).

Mazurek, K. A., N. Rajaratnam, and D. C. Sego (2003), Scour of a cohesive soil by submerged plane turbulent wall jets, *J. Hydraul. Res.*, *41*(2), 195–206.

Misri, R. L., K. G. Ranga Raju, and R. J. Garde (1984), Bed load transport of coarse nonuniform sediments, *J. Hydraul. Eng.*, *110*(3), 312–328, doi:10.1061/(ASCE)0733-9429(1984)110:3(312).

Mitchener, H., and H. Torfs (1996), Erosion of mud-sand mixtures, *J. Coastal Eng.*, *29*, 1–25, doi:10.1016/S0378-3839(96)00002-6.

Moore, W. L., and F. D. Masch (1962), Experiment on the scour resistance of cohesive sediments, *J. Geophys. Res.*, *67*(4), 1437–1446, doi:10.1029/JZ067i004p01437.

Niekerk, A. V., K. R. Vogel, R. L. Slingerland, and J. S. Bridge (1992), Routing of heterogeneous sediments over movable beds: Model development, *J. Hydraul. Eng.*, *118*(2), 246–262, doi:10.1061/(ASCE)0733-9429(1992)118:2(246).

Parker, D. B., T. G. Michel, and J. L. Smith (1995), Compaction and water velocity effects on soil erosion in shallow flows, *J. Irrig. Drain. Eng.*, *121*(2), 170–178, doi:10.1061/(ASCE)0733-9437(1995)121:2(170).

Parker, G. (1990), Surface based bed load transport relation, *J. Hydraul. Res.*, *28*(4), 417–436.

Partheniades, E. (1962), A study of erosion and deposition of cohesive soils in saltwater, Ph.D. thesis, Univ. of Calif., Berkeley.

Partheniades, E. (1965), Erosion and deposition of cohesive soils, *J. Hydraul. Div. Am. Soc. Civ. Eng.*, *91*(1), 105–139.

Partheniades, E. (1966), Closure of erosion and deposition of cohesive soils, *J. Hydraul. Div. Am. Soc. Civ. Eng.*, *92*(3), 79–81.

Partheniades, E., and R. E. Passwell (1970), Erodibility of channels with cohesive boundaries, *J. Hydraul. Eng.*, *96*(HY3), 755–771.

Patel, P. L., and K. G. Ranga Raju (1996), Fractionwise calculation of bed load transport, *J. Hydraul. Res.*, *34*(3), 367–379.

Prior, D. B., and B. D. Bornhold (1986), Sediment transport on subaqueous fan delta slope, Britannia Beach, British Columbia, *Geo Mar. Lett.*, *5*, 217–224, doi:10.1007/BF02233806.

Rahuel, J. L., F. M. Holly, J. P. Chollet, P. Belludi, and G. Yang (1989), Modelling of river bed evolution for bed load sediment mixtures, *J. Hydraul. Eng.*, *115*(11), 1521–1542, doi:10.1061/(ASCE)0733-9429(1989)115:11(1521).

Raudikivi, A. J. (1990), *Loose Boundary Hydraulics*, 3rd ed., chap. 9, pp. 237–296, Pergamon, New York.

Roberts, J. L., R. A. Jepsen, D. Gotthard, and W. Lick (1998), Effect of particle size and bulk density on erosion of quartz particles, *J. Hydraul. Eng.*, *129*(11), 862–871, doi:10.1061/(ASCE)0733-9429(2003)129:11(862).

Robinson, K. M., and G. J. Hanson (1995), Large scale headcut erosion testing, *Trans. ASAE*, *38*(2), 429–434.

Shaikh, A., J. Ruff, and S. Abt (1988), Erosion rate of dispersive and non dispersive clays, *J. Geotech. Eng.*, *114*(5), 589–600.

Simon, A., and J. C. Collison (2001), Pore-water pressure effects on the detachment of cohesive streambeds: Seepage forces and matric suction, *Earth Surf. Processes Landforms*, *26*, 1421–1442, doi:10.1002/esp.287.

Singh, A. K., U. C. Kothyari, and K. G. Ranga Raju (2004), Rapidly varying transient flows in alluvial rivers, *J. Hydraul. Res.*, *42*(5), 473–486.

Temple, D. M., and G. J. Hanson (1994), Head cut development in vegetated earth spillways, *J. Appl. Eng.*, *10*(5), 677–682.

Terzaghi, K., R. B. Pech, and G. Mesri (1996), *Soil Mechanics in Engineering Practice*, 3rd ed., John Wiley, New York.

Ting, C. K. F., J. F. Briaud, H. C. Chen, G. Rao, S. Perugu, and G. Wei (2001), Flume tests for scour in clay at circular piers, *J. Hydraul. Eng.*, *127*(11), 969–978, doi:10.1061/(ASCE)0733-9429(2001)127:11(969).

Torfs, H. (1997), Erosion of mixed cohesive/non cohesive sediments in uniform flow, in *Cohesive Sediments*, edited by N. Burt, R. Parker, and J. Watts, pp. 245–252, John Wiley, Chichester, U. K.

van Ledden, M., W. G. M. van Kesteren, and J. C. Winterwerp (2004), A conceptual framework for the erosion behaviour of sand-mud mixtures, *Cont. Shelf Res.*, *24*, 1–11, doi:10.1016/j.csr.2003.09.002.

van Rijn, L. C. (2007), Unified view of sediment transport by currents and waves: I. Initiation of motion, bed roughness and bed load transport, *J. Hydraul. Eng.*, *133*(6), 649–667.

Wan, C. F., and R. Fell (2004), Investigation of rate of erosion of soils in embankment dams, *J. Geotech. Geoenviron. Eng.*, *130*(4), 373–380, doi:10.1061/(ASCE)1090-0241(2004)130:4(373).

Yang, C. T., A. Molinas, and W. Baosheng (1996), Sediment transport in the Yellow River, *J. Hydraul. Eng.*, *122*(5), 237–244, doi:10.1061/(ASCE)0733-9429(1996)122:5(237).

Zreik, D. A., B. G. Krishappan, J. T. Germaine, and O. S. Madsen (1998), Erosional and mechanical strength of deposited cohesive sediments, *J. Hydraul. Eng.*, *124*(11), 1076–1085, doi:10.1061/(ASCE)0733-9429(1998)124:11(1076).

R. K. Jain and U. C. Kothyari (corresponding author), Department of Civil Engineering, Indian Institute of Technology Roorkee, Roorkee, UA 247667, India. (rajkjain7@rediffmail.com; umeshfce@iitr.ernet.in)